Decoherence in a dynamical quantum phase transition

Sarah Mostame,[1,2] Gernot Schaller,[3] and Ralf Schützhold[2,4,*]
[1]*Max-Planck-Institut für Physik Komplexer Systeme, D-01187 Dresden, Germany*
[2]*Institut für Theoretische Physik, Technische Universität Dresden, D-01062 Dresden, Germany*
[3]*Institut für Theoretische Physik, Technische Universität Berlin, D-10623 Berlin, Germany*
[4]*Fachbereich Physik, Universität Duisburg-Essen, D-47048 Duisburg, Germany*
(Received 19 October 2009; published 8 March 2010)

Motivated by the similarity between adiabatic quantum algorithms and quantum phase transitions, we study the impact of decoherence on the sweep through a second-order quantum phase transition for the prototypical example of the Ising chain in a transverse field and compare it to the adiabatic version of Grover's search algorithm, which displays a first-order quantum phase transition. For site-independent and site-dependent coupling strengths as well as different operator couplings, the results show (in contrast to first-order transitions) that the impact of decoherence caused by a weak coupling to a rather general environment increases with system size (i.e., number of spins or qubits). This might limit the scalability of the corresponding adiabatic quantum algorithm.

DOI: 10.1103/PhysRevA.81.032305 PACS number(s): 03.67.Lx, 03.65.Yz, 75.10.Pq, 64.60.Ht

I. INTRODUCTION

A. Quantum phase transitions

In contrast to thermal phase transitions, which occur when the strength of the thermal fluctuations reaches a certain threshold, during recent years, a different class of phase transitions has attracted the attention of physicists, namely transitions taking place at zero temperature [1]. An analytic nonthermal control parameter such as pressure, magnetic field, or chemical composition is varied to access the transition point. Despite the analytic form of the order parameter, the ground state of a system changes nonanalytically. There, order is changed solely by quantum fluctuations, hence the name quantum phase transition (QPT). Let us consider a quantum system (at zero temperature) described by the Hamiltonian H depending on some external parameter g. At a certain critical value of this parameter, g_c, the system is supposed to undergo a phase transition; that is, the ground state $|\Psi_<(g)\rangle$ of $H(g)$ for $g < g_c$ is strongly different from the ground state $|\Psi_>(g)\rangle$ of $H(g)$ for $g > g_c$. For example, $|\Psi_<(g)\rangle$ and $|\Psi_>(g)\rangle$ could have different global or topological properties (such as magnetization) in the thermodynamic limit. Therefore, a quantum phase transition can also be defined as a nonanalyticity of the ground-state properties of the system as a function of the control parameter. If this singularity arises from a simple level-crossing in the ground state [see Fig. 1(a)], then we have a first-order quantum phase transition. The situation is different for continuous transitions, where a higher-order discontinuity occurs in the ground-state energy. Typically, for any finite-size system, a transition will be rounded into a crossover, which is nothing but an avoided level-crossing in the ground state [see Fig. 1(b)]. Continuous transitions can usually be characterized by an order parameter which is a quantity that is zero in one phase (the disordered phase) and nonzero and possibly nonunique in the other phase (the ordered phase). If the critical point is approached, the spatial correlations of the order parameter fluctuations become long-ranged. Close to the critical point, the correlation length Υ diverges as $\Upsilon^{-1} \propto \Lambda|g - g_c|^{\mathfrak{d}}$, where $\mathfrak{d}$ is a critical exponent and Λ is an inverse length scale of the order of the inverse lattice spacing. Let Δ denote the smallest energy excitation gap above the ground state. In most cases, it has been found [1] that, as g approaches g_c, Δ vanishes as $\Delta \propto \Upsilon^{-z} \propto \Lambda^z|g - g_c|^{\mathfrak{d}z}$, where z is the dynamic critical exponent. This poses a scalability problem for adiabatic ground-state preparation schemes (see below), because these require a nonvanishing energy gap Δ.

B. Adiabatic quantum computation

Unfortunately, the actual realization of usual sequential quantum algorithms (where a sequence of quantum gates is applied to some initial quantum state; see, e.g., [2]) goes along with the problem that errors accumulate over many operations and the resulting decoherence tends to destroy the fragile quantum features needed for computation. Therefore, adiabatic quantum algorithms have been suggested [3], where the solution to a problem is encoded in the (unknown) ground state of a (known) Hamiltonian. Since there is evidence in adiabatic quantum computing that the ground state is more robust against decoherence—the ground state cannot decay and phase errors do not play any role, that is, errors can only result from excitations [4,5]—this scheme offers fundamental advantages compared to sequential quantum algorithms, provided there is a sufficiently cold reservoir. Suppose we have to solve a problem that may be reformulated as preparing a quantum system in the ground state of a Hamiltonian H_f. The adiabatic theorem [6] then provides a straightforward method to solve this problem: Prepare the quantum system in the (known and easy-to-prepare) ground state of another Hamiltonian H_0. Apply H_0 to the system and slowly modify it to H_f. For a nonvanishing time-dependent energy gap, the adiabatic theorem ensures that, if this has been done slowly enough, the system will end up in a state close to the ground state of H_f. Therefore, a measurement of the final state will yield a solution of the problem with high probability.

*ralf.schuetzhold@uni-due.de

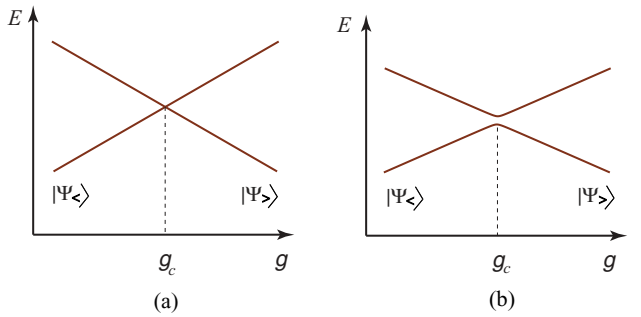

FIG. 1. (Color online) Sketch of the lowest eigenvalues of a Hamiltonian $H(g)$ as a function of some external parameter g for a first-order quantum phase transition. At the critical point $g = g_c$, the ground state changes from $|\Psi_<(g)\rangle$ to $|\Psi_>(g)\rangle$: (a) a level-crossing and (b) an avoided level-crossing.

Furthermore, adiabatic quantum algorithms display a remarkable similarity with sweeps through quantum phase transitions [7,8]. For all interesting systems discussed later in this article, adiabatic quantum computation inherently brings the quantum system near a point that is similar to the critical point in a quantum phase transition. As an example for the deformation of the Hamiltonian, one can consider the linear interpolation path between these two Hamiltonians

$$H(g) = [1 - g(t)]H_0 + g(t)H_f, \tag{1}$$

with $g(0) = 0$ and $g(T) = 1$, where T is the total evolution time or the *run time* of the algorithm. We prepare the ground state of H_0 at time $t = 0$, and then the state evolves from $t = 0$ to T according to the Schrödinger equation. At time T, we measure the state. According to the adiabatic theorem, if there is a nonzero gap between the ground state and the first excited state of $H(g)$ for all $g \in [0, 1]$ then the success probability of the algorithm approaches 1 in the limit $T \to \infty$. How large T should actually be is roughly given by [9]

$$T \gg \frac{\max_{g\in[0,1]} \left|\langle 1, g|\frac{dH(g)}{dg}|0, g\rangle\right|}{\min_{g\in[0,1]}[E_1(g) - E_0(g)]^2}, \tag{2}$$

where $E_0(g)$ is the lowest eigenvalue of $H(g)$, $E_1(g)$ is the second-lowest eigenvalue, and $|0, g\rangle$ and $|1, g\rangle$ are the corresponding eigenstates, respectively (for a more detailed discussion, see, e.g., [10,11]). Somewhere on the way from the simple initial configuration H_0 to the unknown solution of some problem encoded in H_f there is typically a critical point which bears strong similarities to a quantum phase transition. At this critical point the fundamental gap (which is sufficiently large initially and finally) becomes very small (see, e.g., Fig. 2). Near the position of the minimum gap, the ground state changes more drastically than in other time intervals of the interpolation. In the continuum limit, one would generally expect that the minimum value of the fundamental gap in adiabatic computation vanishes identically and that the ground state changes nonanalytically at the critical point. This is similar to what happens in a quantum phase transition when g approaches g_c. Based on this similarity, it seems [8] that adiabatic quantum algorithms corresponding to second-order quantum phase transitions should be advantageous compared to isolated avoided level crossings (which are analogous to first-order transitions). A brief review of this idea is given in the following section.

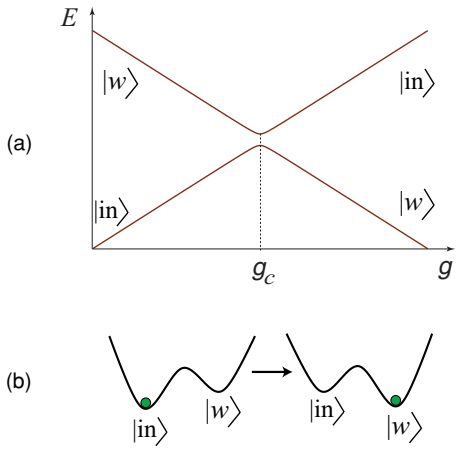

FIG. 2. (Color online) (a) Sketch of the two lowest-energy eigenvalues of the Grover Hamiltonian. (b) In the continuum limit, this corresponds to the time evolution of the energy landscape for a first-order transition. The (green) dot in the energy landscape denotes the ground state.

II. EXAMPLES

A. First-order transition: Grover's algorithm

An adiabatic version of Grover's algorithm [12] is defined by the Hamiltonian

$$H(g) = (1 - g)H_0 + g H_f, \tag{3}$$

where the initial Hamiltonian is given by $H_0 = \mathbf{1} - |\text{in}\rangle\langle\text{in}|$ with the initial superposition state $|\text{in}\rangle = \sum_{x=0}^{D-1} |x\rangle / \sqrt{D}$, and $D \equiv 2^N$ denotes the dimension of the Hilbert space for N qubits. The final Hamiltonian reads $H_f = \mathbf{1} - |w\rangle\langle w|$, where $|w\rangle$ denotes the marked state. In this case, the commutator is very small: $[H_0, H_f] = (|\text{in}\rangle\langle w| - |w\rangle\langle\text{in}|)/\sqrt{D}$. One can nearly diagonalize both Hamiltonians simultaneously, and the g-dependent spectrum consists of nearly straight lines, except near $g_c = 1/2$, where we have an avoided level-crossing (see Fig. 2). In the continuum limit of $N \to \infty$, this corresponds to a first-order quantum phase transition from $|\text{in}\rangle = |\to \cdots \to\rangle$ to $|w\rangle = |\uparrow\downarrow \cdots \uparrow\downarrow\downarrow\rangle$, for example, at the critical point $g_c = 1/2$. Such a first-order transition is characterized by an abrupt change of the ground state ($|\text{in}\rangle$ for $g < g_c$ and $|w\rangle$ for $g > g_c$), resulting in a discontinuity of a corresponding order parameter (see Fig. 3),

$$\langle\psi_0(g)|\,\frac{dH}{dg}\,|\psi_0(g)\rangle = \frac{dE_0}{dg}. \tag{4}$$

In contrast to the conventional order parameters, for linear interpolations in Eq. (3) the operator dH/dg treats both phases symmetrically. Since $[H_I, H_F] \neq 0$ (for nontrivial systems), dH/dg is off-diagonal in either phase and thereby plays an equivalent role (e.g., magnetization).

First-order quantum phase transitions are typically associated with an energy landscape as pictured in Fig. 2, where the two competing ground states are separated by an energy barrier throughout the interpolation. In order to stay in the

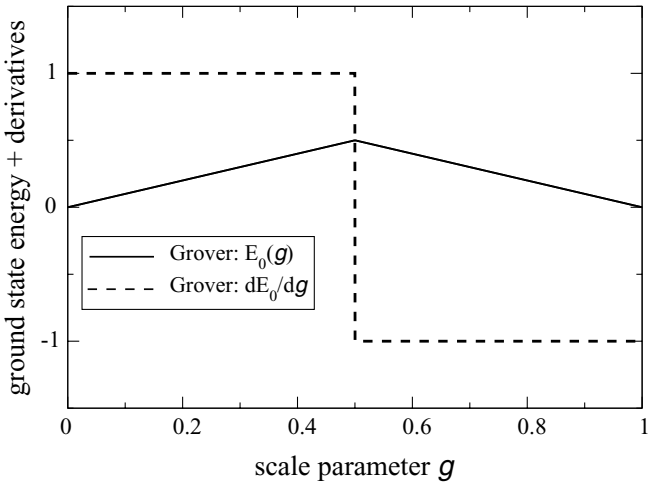

FIG. 3. The ground-state energy of the Grover Hamiltonian and its first-order derivative. The discontinuity in the first-order derivative of the ground state suggests the first-order quantum phase transition in adiabatic quantum search algorithm.

ground state, the system has to tunnel through the barrier between the initial ground state $|\text{in}\rangle$ and the final ground state $|w\rangle$ during the quantum phase transition. The natural increase in the strength of the barrier with the system size N yields a tunneling time that scales exponentially with the system size. Specifically, the optimal run time for the adiabatic search algorithm behaves as $T = O(\sqrt{D}) = O(2^{N/2})$ [12]. The observation that this first-order QPT is associated with an exponentially small energy gap right at the avoided crossing can be generalized [13] to local Hamiltonians: The two-dimensional subspace of the avoided crossing is spanned by the eigenstates $|w_<(g)\rangle$ and $|w_>(g)\rangle$ that become degenerate at $g = g_c$. Due to their macroscopic distinguishability, the overlap between these states is exponentially small, which for local Hamiltonians also transfers to the matrix element $\langle w_<(g_c)|\, H(g_c)\, |w_>(g_c)\rangle = O\,(\exp\{-D\})$. Consequently, one can also conclude from the eigenvalues of $H(g)$ in this two-dimensional subspace that the minimum energy gap will become exponentially small in this case.

Therefore, the abrupt change of the ground state and the energy barrier between the initial and final ground states suggest that the first-order transitions are not the best choice for the realization of adiabatic quantum algorithms [8]. Thus, it would be relevant to study higher-order quantum phase transitions for this purpose.

B. Second-order transition: Ising model

The one-dimensional quantum Ising model is one of the two paradigmatic examples [1] of second-order quantum phase transition (the other being the Bose-Hubbard model). Of these two, only the former model is exactly solvable [1,14]; the Ising model in a transverse field is a special case of the XY model (which can also be diagonalized completely). This model has been employed in the study of quantum phase transitions and percolation theory [1], spin glasses [1,15], as well as quantum annealing [16–18]. Although its Hamiltonian is quite simple, the Ising model is rich enough to display most of the basic phenomena near quantum critical points. Furthermore, the transverse Ising model can also be used to study the order-disorder transitions driven by quantum fluctuations at zero temperature [1,16]. Finally, two-dimensional generalizations of the Ising model can be mapped onto certain adiabatic quantum algorithms (see, e.g., [19]). However, due to the evanescent excitation energies, such a phase transition is rather vulnerable to decoherence, which must be taken into account [20].

The one-dimensional transverse Ising chain of N spins exhibits a time-dependent nearest-neighbor interaction $g(t)$ plus transverse field $B(t) = 1 - g(t)$:

$$H_{\text{sys}}(t) = -\sum_{j=1}^{N} \left\{[1 - g(t)]\sigma_j^x + g(t)\sigma_j^z\sigma_{j+1}^z\right\}, \qquad (5)$$

where $\boldsymbol{\sigma}_j = (\sigma_j^x, \sigma_j^y, \sigma_j^z)$ are the spin-1/2 Pauli matrices acting on the jth qubit, and periodic boundary conditions $\boldsymbol{\sigma}_{N+1} = \boldsymbol{\sigma}_1$ are imposed. This Hamiltonian is invariant under a global 180° rotation around the σ_j^x axes (bit flip), which transforms all qubits according to $\sigma_j^z \to -\sigma_j^z$. Choosing $g(0) = 0$ and $g(T) = 1$, where T is the evolution time, the quantum system evolves from the unique paramagnetic state $|\text{in}\rangle = |\rightarrow\rightarrow\rightarrow\cdots\rangle$ through a second-order quantum phase transition (see Fig. 4) at $g_{\text{cr}} = 1/2$ to the symmetrized combination in the twofold degenerate ferromagnetic subspace (see also Fig. 5):

$$|w\rangle = \frac{|\uparrow\uparrow\uparrow\cdots\rangle + |\downarrow\downarrow\downarrow\cdots\rangle}{\sqrt{2}}. \qquad (6)$$

At the critical point g_{cr}, the excitation gap vanishes (in the thermodynamic limit $N \to \infty$) and the response time diverges. As a result, driving the system through its quantum critical point at a finite sweep rate entails interesting nonequilibrium phenomena such as the creation of topological defects (i.e., kinks [21]).

Since the initial ground state $|\text{in}\rangle$ reflects the bit-flip invariance of Hamiltonian (5), whereas the final ground-state subspace $|\uparrow\cdots\uparrow\rangle$ and $|\downarrow\cdots\downarrow\rangle$ breaks this symmetry, we have a symmetry-breaking quantum phase transition.

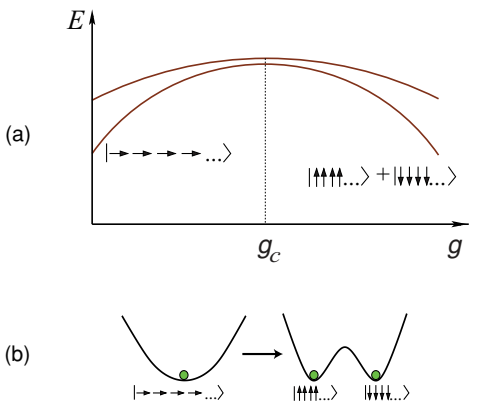

FIG. 4. (Color online) (a) Sketch of the two lowest energy levels of the Ising Hamiltonian given in Eq. (5) (b) The time evolution of the energy landscape for a second-order transition. A symmetry-breaking transition corresponds to the deformation of the energy landscape. The green dot in the energy landscape denotes the ground state.

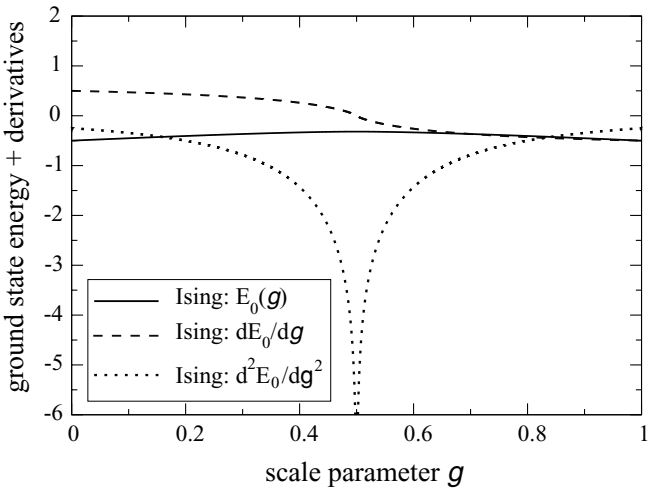

FIG. 5. The ground-state energy density for the Ising model and its first and second derivatives in the infinite size limit. The discontinuity in the second-order derivative of the ground state suggests a second-order quantum phase transition.

Typically, such a symmetry-breaking change of the ground state corresponds to a second-order phase transition [8]. For such a transition, the ground state changes continuously and the energy barrier observed in first-order transitions is absent: Initially, there is a unique ground state, but at the critical point, this ground state splits into two degenerate ground states which are the mirror image of each other. Therefore, the ground state does not change abruptly in this situation and the system does not need to tunnel through a barrier in order to stay in the ground state [see Fig. 4(b)]. Consequently, we expect in this case that a closed quantum system should more easily find its way from the initial to the final ground state. This expectation is confirmed in later sections of this article. Since the minimum gap behaves as $O(1/N)$, the optimal run time to stay in the ground state scales polynomially for the Ising model.

C. Mixed case

Looking at Fig. 4, it seems that a symmetry-breaking quantum phase transition typically corresponds to a second-order phase transition, but there are counterexamples. Consider the more complicated energy landscape [22] in Fig. 6. In spite of the mirror symmetry of the energy landscape, there is a tunneling barrier throughout the interpolation. An analytic example for a symmetry-breaking first-order transition [22] is given by a combination of the initial Hamiltonian from the

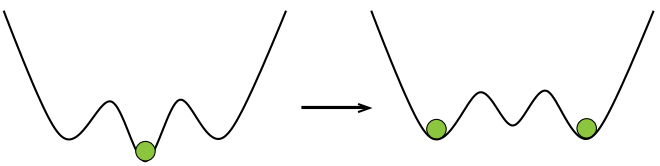

FIG. 6. (Color online) Sketch of the time evolution of the energy landscape for a symmetry-breaking quantum phase transition which is of first order. The (green) dot denotes the ground state.

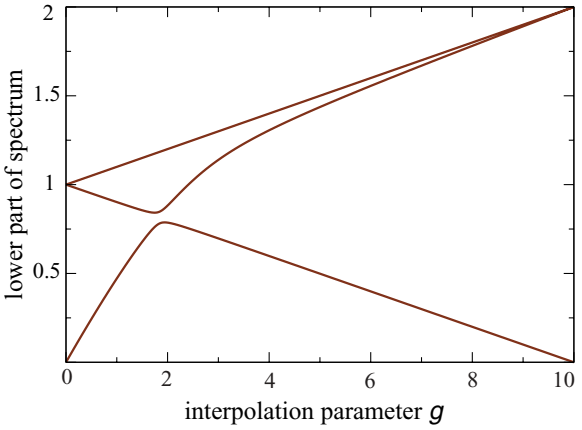

FIG. 7. (Color online) Sketch of the lowest eigenvalues of Hamiltonian (7). One can clearly see that the spectrum displays an avoided level-crossing at the critical point, thus corresponding to a first-order transition [22].

Grover problem with the final Hamiltonian of the Ising model:

$$H_0 = \mathbf{1} - |\mathrm{in}\rangle\langle\mathrm{in}|, \quad H_\mathrm{f} = \frac{1}{2}\sum_{j=1}^{N}\left(\mathbf{1} - \sigma_j^z\sigma_{j+1}^z\right), \qquad (7)$$

where H_f has been shifted and scaled in order to preserve positive definiteness. Even though this Hamiltonian possesses the same bit-flip symmetry as the Ising model, its level structure displays an avoided level-crossing at the critical point; that is, it corresponds to a first-order phase transition with a jump between the initial and the final ground state(s) (see Fig. 7).

It can also be shown analytically that the fundamental gap of the combined Hamiltonian $H(g) = (1-g)H_0 + gH_\mathrm{f}$ vanishes exponentially with the system size (i.e., the number of qubits; see, e.g., [23,24]).

III. DECOHERENCE IN THE ADIABATIC LIMIT

In all of the preceding examples, we have seen that at the critical point at least some energy levels become arbitrarily close and, thus, the response times diverge (in the continuum limit). Consequently, during the sweep through such a phase transition by means of a time-dependent external parameter, small external perturbations or internal fluctuations become strongly amplified, leading to many interesting effects (see, e.g., [25–31]). One of them is the anomalously high susceptibility to decoherence (see also [32]). Due to the convergence of the energy levels at the critical point, even low-energy modes of the environment may cause excitations and thus perturb the system. Based on the similarity between the quantum adiabatic algorithms and the critical phenomena, we have argued that adiabatic quantum algorithms corresponding to the higher-order quantum phase transitions should be advantageous in comparison to those of first order for closed quantum systems. This article aims at generalizations to these findings when the impact of decoherence is considered.

In order to study the impact of decoherence, we consider an open system described by the total Hamiltonian $H(t)$ which can be split up into that of the closed system H_sys and the bath

$H_{\rm bath}$ acting on independent Hilbert spaces $\mathcal{H}_{\rm sys} \otimes \mathcal{H}_{\rm bath} = \mathcal{H}$:

$$H(t) = H_{\rm sys}(t) + H_{\rm bath} + \lambda H_{\rm int}, \tag{8}$$

plus an interaction $\lambda H_{\rm int}$ between the two, which is supposed to be weak ($\lambda \ll 1$) in the sense that it does not drastically perturb the state of the system. Note that the change of the bath caused by the interaction need not be small. To describe the evolution of the combined quantum state $|\Phi(t)\rangle \in \mathcal{H}$, we expand it using the instantaneous system energy eigenbasis $H_{\rm sys}(t)\,|\psi_s(t)\rangle = E_s(t)\,|\psi_s(t)\rangle$, via

$$|\Phi(t)\rangle = \sum_s a_s(t)\,|\psi_s(t)\rangle \otimes |\alpha_s(t)\rangle, \tag{9}$$

where a_s are the corresponding amplitudes and $|\alpha_s\rangle \in \mathcal{H}_{\rm bath}$ denote the associated (normalized but not necessary orthogonal) states of the reservoir. Insertion of this expansion into the Schrödinger equation $i|\dot{\Phi}(t)\rangle = H(t)|\Phi(t)\rangle$ yields ($\hbar = 1$)

$$\frac{\partial}{\partial t}(a_s e^{-i\varphi_s}) = e^{-i\varphi_s} \sum_{r\neq s} a_r \left(\frac{\langle\psi_s|\dot{H}_{\rm sys}|\psi_r\rangle}{\Delta E_{sr}} \langle\alpha_s|\alpha_r\rangle - i\,\langle\alpha_s|\langle\psi_s|\lambda H_{\rm int}|\psi_r\rangle|\alpha_r\rangle \right) \tag{10}$$

with the energy gaps $\Delta E_{sr}(t) = E_s(t) - E_r(t)$ of the system and the total phase (including the Berry phase)

$$\varphi_s(t) = -\int_0^t dt' \big[E_s(t') + H^{ss}_{\rm bath}(t') + \lambda H^{ss}_{\rm int}(t') - i\,\langle\psi_s(t')|\dot{\psi}_s(t')\rangle - i\,\langle\alpha_s(t')|\dot{\alpha}_s(t')\rangle \big] \tag{11}$$

with the energy shift $H^{sr}_{\rm int} = \langle\alpha_s|\,\langle\psi_s|\,H_{\rm int}\,|\psi_r\rangle\,|\alpha_r\rangle$, $H^{sr}_{\rm bath} = \langle\alpha_s|\,H_{\rm bath}\,|\alpha_r\rangle$. Evidently, there are two contributions for transitions in the Hilbert space, $\mathcal{H}_{\rm sys}$, of the system:

1. The first term on the right-hand side of Eq. (10) describes the transitions caused by a nonadiabatic evolution [9]. Note, however, that the factor $\langle\alpha_s|\alpha_r\rangle$ and the additional phases in Eq. (11) give rise to modifications in the adiabatic expansion.
2. The last term in Eq. (10) directly corresponds to transitions caused by the interaction of the quantum system with its environment.

Since we are mainly interested in the impact of the coupling to the bath, we assume a perfectly adiabatic evolution of the system itself; that is, without the coupling to the environment $\lambda = 0$, the system would stay in its ground state. Thus, the only decoherence channel available is heating (i.e., excitations); the phase damping and decay channels, for example, play no major role here. Considering the adiabatic condition

$$\langle\psi_s|\,\dot{H}_{\rm sys}\,|\psi_r\rangle \ll (\Delta E_{sr})^2\,, \tag{12}$$

the first term in Eq. (10) is negligible and the second one dominates. Starting in the system's ground state $a_0(t=0) = 1$, which is relevant for adiabatic quantum computation, the excitations $s > 0$ caused by the weak interaction $\lambda H_{\rm int}$ with the bath

$$\mathfrak{A}_s \equiv a_s(T)\exp\{-i\varphi_s(T)\} \tag{13}$$

can be calculated via response theory; that is, the solution of Eq. (10) is to first order in $\lambda \ll 1$ given by

$$\mathfrak{A}_s \approx -i\int_0^T dt e^{i\Delta\varphi_{0s}}\,\langle\alpha_s|\,\langle\psi_s|\,\lambda H_{\rm int}\,|\psi_0\rangle\,|\alpha_0\rangle\,, \tag{14}$$

where $\Delta\varphi_{rs} = \varphi_r(t) - \varphi_s(t)$. This is a rather general result.

In the following, after a brief review of the impact of decoherence on the sweep through a first-order quantum phase transition [33] in Sec. IV, in Sec. V we study the impact of decoherence due to a general reservoir for the quantum Ising chain in a transverse field, which is considered a prototypical example for a second-order quantum phase transition.

IV. DECOHERENCE IN THE ADIABATIC GROVER SEARCH

Let us consider the Grover model (3), weakly coupled to a bath, where we can assume the following expansion of the interaction Hamiltonian [33]:

$$\lambda H_{\rm int} = \lambda \sum_{j=1}^N \boldsymbol{\sigma}_j \cdot \boldsymbol{A}_j + \lambda^2 \sum_{\ell,j=1}^N \boldsymbol{\sigma}_\ell \cdot \boldsymbol{B}_{\ell j} \cdot \boldsymbol{\sigma}_j + O(\lambda^3), \tag{15}$$

where $\lambda \ll 1$ and $\boldsymbol{\sigma}_j(t) = (\sigma_j^x(t), \sigma_j^y(t), \sigma_j^z(t))$ is the vector of Pauli matrices in the interaction picture with the corresponding bath operators $\boldsymbol{A}_j(t)$, $\boldsymbol{B}_{\ell j}(t)$, and so forth. Recalling the adiabatic version of Grover's search algorithm in Eq. (3), at the beginning of the evolution the system has to be prepared in the ground state $|{\rm in}\rangle = \sum_{x=0}^{D-1} |x\rangle/\sqrt{D}$. This approach also requires that the initial full-density operator can be initialized as a direct product

$$\varrho(0) = \varrho_{\rm sys}(0) \otimes \varrho_{\rm bath}(0) \tag{16}$$

(i.e., system and environment are not entangled at the beginning). Since the adiabaticity condition in the weak-coupling limit for the open system dynamics is still in leading order the same as that for the closed system, similar to the discussions in the previous section, one can assume perfect adiabatic evolution of the unperturbed system and, hence, only consider perturbations due to the interaction with the environment.

The spectrum of Grover Hamiltonian (3) consists of the ground state $|\psi_0(g)\rangle$ and the first excited state $|\psi_1(g)\rangle$, which come very close ($\Delta E_{\rm min} = 1/\sqrt{D}$) at $g_c = 1/2$, whereas all other states $|\psi_{k>1}(g)\rangle$ are degenerate and well separated from the ground state by an energy gap of order 1. Since the temperature and, hence, the energies available in the environment must be much smaller than that gap of order 1 (in order to prepare the initial ground state), transitions from the ground state to these states $|\psi_{k>1}(g)\rangle$ are exponentially suppressed. Thus, the final probability of the transitions to the first excited state [33],

$$|\mathfrak{A}_s|^2 \approx \lambda^2 \sum_{\substack{\ell,j=1\\ \mu,\nu=x,y,z}}^N \int_0^T dt_1 \int_0^T dt_2 \left\langle A_\ell^\mu(t_1) A_j^\nu(t_2)\right\rangle \times \langle w^\perp|\sigma_\ell^\mu(t_1)\,|w\rangle\,\langle w|\,\sigma_j^\nu(t_2)|w^\perp\rangle, \tag{17}$$

provides a good measure for the success probability, which corresponds to $|\mathfrak{A}_s|^2 \ll 1$. It can be shown [33] that the contributions proportional to $B_{\ell j}$ do not contribute to second

order in λ. In this equation, $|w\rangle$ denotes the marked state for Grover's problem [see Eq. (3)], and $|w^\perp\rangle$ is the state orthogonal to $|w\rangle$ in the subspace spanned by $|w\rangle$ and $|\mathrm{in}\rangle$. Expression (17) demonstrates that both system and reservoir properties affect the excitation amplitude. Of the system matrix elements $\langle w^\perp|\sigma_j^\mu(t)|w\rangle$, only those with $\mu = x, z$ contribute (for large $D = 2^N \gg 1$, the $\mu = y$ term is suppressed by a factor $1/\sqrt{D}$)

$$\langle w^\perp|\sigma_j^x(t)\,|w\rangle \approx -\frac{1-g(t)}{\sqrt{D}\Delta E(t)} \exp\left\{-i\int_0^t dt'\Delta E(t')\right\}, \tag{18}$$

for large N and $\Delta E(t) = \sqrt{1-4g(t)[1-g(t)](1-1/D)}$. It is the same for $\langle w^\perp|\sigma_j^z(t)\,|w\rangle$ apart from an additional sign $(-1)^{w_j+1}$, where w_j is the jth bit of w; that is, $|w\rangle$ is an eigenstate of the operators σ_j^z with eigenvalues $(-1)^{w_j}$.

Assuming a stationary reservoir $[H_{\mathrm{bath}}, \varrho_{\mathrm{bath}}] = 0$ (which does not necessarily imply a bath in thermal equilibrium) allows for a Fourier decomposition of the bath correlation function

$$\left\langle A_\ell^\mu(t_1)A_j^\nu(t_2)\right\rangle = \int_{-\infty}^{+\infty} d\omega\, e^{-i\omega(t_1-t_2)} f_{\ell j}^{\mu\nu}(\omega), \tag{19}$$

where $f_{\ell j}^{\mu\nu}(\omega)$ depends on the spectral distribution of the bath modes, the temperature, and so forth.

For example, for a bosonic bath in thermal equilibrium and coupling operators $A_j^\mu \propto \sum_k [h_k a_k + h_k^* a_k^\dagger]$ (as used, e.g., in the spin-boson model), we would for an inverse bath temperature β obtain a Fourier decomposition such as [34]

$$f_{\ell j}^{\mu\nu}(\omega) \propto \frac{J(|\omega|)}{|1-e^{-\beta\omega}|} = J(|\omega|)\left[\frac{1}{e^{\beta|\omega|}-1} + \Theta(\omega)\right], \tag{20}$$

where $\Theta(\omega)$ is the step function equal to 1 for $\omega > 0$ and 0 for $\omega < 0$. The spectral density is denoted by $J(\omega)$, which is often parametrized as [35]

$$J(\omega) = 2\vartheta\omega_{\mathrm{ph}}^{1-\epsilon}\omega^\epsilon e^{-\omega/\omega_{\mathrm{c}}}, \tag{21}$$

where $0 \leqslant \epsilon < 1$ corresponds to the sub-Ohmic, $\epsilon = 1$ to the Ohmic, and $\epsilon > 1$ to the super-Ohmic case.

Insertion of Eqs. (18) and (19) into Eq. (17) yields

$$|\mathfrak{A}_s|^2 \approx \lambda^2 \int d\omega \sum_{\ell,j=1}^{N} f_{\ell j}^{xx}(\omega) \times \left|\int_0^T dt \frac{1-g(t)}{\sqrt{D}\Delta E(t)} \exp\left\{i\omega t + i\int_0^t dt'\Delta E(t')\right\}\right|^2 \tag{22}$$

plus similar terms including $f_{\ell j}^{xz}$, $f_{\ell j}^{zx}$, and $f_{\ell j}^{zz}$ with the associated signs (-1) and $(-1)^{w_j}$ for x and z, respectively [33]. In order to evaluate the time integrations, it is useful to distinguish different domains of ω:

1. For large frequencies $|\omega| \gg \Delta E_{\mathrm{min}}$, the time integral can be calculated via the saddle-point approximation. The saddle points t_ω^* are given by a vanishing derivative of the exponent

$$\omega + \Delta E(t_\omega^*) = 0, \tag{23}$$

which corresponds to energy conservation. Hence, large positive frequencies $\omega \gg \Delta E_{\mathrm{min}}$ do not contribute at all, which is quite natural (and corresponds to the transfer of a large energy from the system to the reservoir).

2. The saddle-point approximation cannot be applied for small frequencies $\omega = O(\Delta E_{\mathrm{min}})$ and energy conservation is also not well defined. In this case, one might estimate an upper bound for the time integral by omitting all phases.

These domains altogether yield

$$|\mathfrak{A}_s|^2 \approx \lambda^2 D \int_{-\Delta E_{\mathrm{min}}}^{+\Delta E_{\mathrm{min}}} d\omega f(\omega) + \frac{\pi\lambda^2}{2D}\int_{\Delta E_{\mathrm{min}}}^{1} d\omega \frac{f(-\omega)}{\omega^2\dot{g}(t_\omega^*)}, \tag{24}$$

where $f(\omega)$ is the appropriate sum of the $f_{\ell j}^{xx}$, $f_{\ell j}^{xz}$, $f_{\ell j}^{zx}$, and $f_{\ell j}^{zz}$ contributions. The second term of the preceding equation depends on the interpolation function $g(t)$. Considering three scenarios [10]

$$\text{(a)}\ddot{g} = 0, \quad \text{(b)}\dot{g} \propto \Delta E, \quad \text{(c)}\dot{g} \propto \Delta E^2,$$

the second integrand scales as

$$\text{(a)}\frac{Df(-\omega)}{\omega^2}, \quad \text{(b)}\frac{\sqrt{D}f(-\omega)}{\omega^3}, \quad \text{(c)}\frac{f(-\omega)}{\omega^4},$$

respectively. In all of these cases, the bath modes with large frequencies $|\omega| \gg \Delta E_{\mathrm{min}}$ do not cause problems in the large-$N(D)$ limit, since the spectral function $f(-\omega)$ is supposed to decrease for large $|\omega|$ as the bath does not contain excitations with large energies—the environment is cold enough [compare also Eq. (20)]. Therefore, the low-energy modes of the reservoir $\omega = O(\Delta E_{\mathrm{min}})$ give the potentially dangerous contributions. Independent of the dynamics $g(t)$, both the first integral and the lower limit of the second integral yield the same order of magnitude [33]:

$$|\mathfrak{A}_s|^2 \approx \lambda^2 \frac{f\,[O(\Delta E_{\mathrm{min}})]}{\Delta E_{\mathrm{min}}}. \tag{25}$$

Since ΔE_{min} decreases as $1/\sqrt{D}$ in the large-D limit, the spectral function $f(\omega)$ must vanish in the infrared limit as ω or even faster in order to keep the error $|\mathfrak{A}_s|^2$ under control. Thus, one can conclude that the spectral function $f(\omega)$ of the bath provides a criterion that favors or disfavors certain physical implementations. If $f(\omega)$ vanishes in the infrared limit faster than ω [compare also Eq. (21)], the computational error does not grow with increasing system size—the quantum computer is *scalable*. This result has already been derived in [33] with a slightly different formalism.

V. RESULTS: DECOHERENCE IN THE TRANSVERSE ISING CHAIN

As we see below, the situation may be very different for second-order transitions compared to first-order transitions. These investigations are particularly relevant in view of the announcement (see, e.g., the discussion in [19]) regarding the construction of an adiabatic quantum computer with 16 qubits in the form of a two-dimensional Ising model.

First of all, we briefly review the main steps [1] of the analytic diagonalization of $H_{\rm sys}$, where we switch temporarily to the Heisenberg picture for convenience. The set of N qubits in Eq. (5) can be mapped to a system of N spinless fermions c_j via the Jordan-Wigner transformation [36] given by

$$\begin{aligned}\sigma_j^x(t) &= 1 - 2c_j^\dagger(t)c_j(t),\\ \sigma_j^z(t) &= -\prod_{\ell<j}[1-2c_\ell^\dagger(t)c_\ell(t)][c_j(t)+c_j^\dagger(t)],\end{aligned} \tag{26}$$

where $\boldsymbol{\sigma}_j(t)$ indicates the Pauli operators in the Heisenberg picture $\boldsymbol{\sigma}_j(t) = \mathcal{U}_{\rm sys}^\dagger(t)\boldsymbol{\sigma}_j\mathcal{U}_{\rm sys}(t)$, where $\mathcal{U}_{\rm sys}(t)$ is the unitary time-evolution operator of the system. It is easy to verify that the fermionic operators' anticommutation relations are satisfied

$$\{c_\ell, c_j^\dagger\} = \delta_{\ell j}, \quad \{c_\ell, c_j\} = \{c_\ell^\dagger, c_j^\dagger\} = 0. \tag{27}$$

Insertion of Eq. (26) into the system Hamiltonian in Eq. (5) yields, in the subspace of an even particle number,

$$\begin{aligned}H_{\rm sys}(t) = -\sum_{j=1}^{N}\{&[1-g(t)](1-2c_j^\dagger c_j)\\ &+ g(t)(c_{j+1}c_j + c_{j+1}^\dagger c_j + c_j^\dagger c_{j+1} + c_j^\dagger c_{j+1}^\dagger)\},\end{aligned} \tag{28}$$

where the time dependency of c_j has been dropped for brevity. This fermionic Hamiltonian has terms that violate the fermion conservation number, $c_{j+1}c_j$ and $c_j^\dagger c_{j+1}^\dagger$. This bilinear form can now be diagonalized by a Fourier transformation

$$c_j(t) = \frac{1}{\sqrt{N}}\sum_k \tilde{c}_k(t)\, e^{-ik(ja)}, \tag{29}$$

followed by a Bogoliubov transformation [37]. Here a is lattice spacing. The Bogoliubov transformation

$$\tilde{c}_k(t) = u_k(t)\gamma_k + i v_k^*(t)\gamma_{-k}^\dagger \tag{30}$$

maps the Hamiltonian into a new set of fermionic operators γ_k whose number is conserved. The same anticommutation relations as in Eq. (27) are also satisfied by γ_k and $\gamma_k^\dagger$:

$$\{\gamma_k, \gamma_{k'}^\dagger\} = \delta_{kk'}, \quad \{\gamma_k, \gamma_{k'}\} = \{\gamma_k^\dagger, \gamma_{k'}^\dagger\} = 0. \tag{31}$$

Since these fermionic operators are supposed to be time-independent, the Bogoliubov coefficients u_k and v_k must satisfy [21] the equations of motion

$$\begin{aligned}i\frac{du_k}{dt} &= \alpha_k(t)u_k(t) + \beta_k(t)v_k(t),\\ i\frac{dv_k}{dt} &= -\alpha_k(t)v_k(t) + \beta_k(t)u_k(t),\end{aligned} \tag{32}$$

where $\alpha_k = 2 - 4g(t)\cos^2(ka/2)$, $\beta_k = 2g(t)\sin(ka)$. For an adiabatic evolution $\langle\psi_s|\dot{H}_{\rm sys}|\psi_r\rangle \ll (\Delta E_{sr})^2$, these equations of motion can be solved approximately

$$\begin{aligned}u_k(t) &\approx \frac{\alpha_k(t)+\mathscr{E}_k(t)}{\mathcal{N}_k}\exp\left\{-i\int_0^t dt'\mathscr{E}_k(t')\right\},\\ v_k(t) &\approx \frac{\beta_k(t)}{\mathcal{N}_k}\exp\left\{-i\int_0^t dt'\mathscr{E}_k(t')\right\},\end{aligned} \tag{33}$$

with the normalization $\mathcal{N}_k = \sqrt{2\mathscr{E}_k^2 + 2\alpha_k\mathscr{E}_k}$ ensuring $|u_k|^2 + |v_k|^2 = 1$ and the single-particle energies

$$\mathscr{E}_k(t) = 2\sqrt{1-4g(t)[1-g(t)]\cos^2(ka/2)}. \tag{34}$$

All the excitation energies $\mathscr{E}_k$ take their minimum values $\mathscr{E}_k^{\rm min} = 2|\sin(ka/2)|$, at the critical point $g_{\rm cr} = 1/2$. The pseudomomenta ka take half-integer values $ka \in (1+2\mathbb{Z})\pi/N$: $|ka| < \pi$. In view of the k spectrum, the minimal gap between the ground state and the first excited state scales as $\Delta E_{\rm min} = O(1/N)$. Finally, Hamiltonian (5) in the subspace of an even number of quasiparticles reads

$$H_{\rm sys}(t) = \sum_k \mathscr{E}_k(t)\left(\gamma_k^\dagger\gamma_k - \frac{1}{2}\right) \tag{35}$$

with fermionic creation and annihilation operators $\gamma_k^\dagger, \gamma_k$. Hence, its (instantaneous) ground state contains no fermionic quasiparticles $\forall_k : \gamma_k|\psi_0(t)\rangle = 0$. Without the environment, the number of fermionic quasiparticles $\gamma_k^\dagger\gamma_k$ would be conserved and the system would stay in an eigenstate (e.g., ground state) for an adiabatic evolution. The coupling to the bath, however, may cause excitations and, thus, the creation of quasiparticles due to decoherence.

Of course, the impact of decoherence depends on the properties of the bath and its interaction with the system (decoherence channels). In the following, we study three different decoherence channels. However, in all of these different cases, we do not specify the bath $H_{\rm bath}$ in much detail for the purpose of deriving generally applicable results.

A. Uniform coupling strengths

Let us first consider an interaction $\lambda H_{\rm int}$ which is always present. In the Hamiltonian $H_{\rm sys}$ in Eq. (5), the transverse field $B(t) = 1 - g(t)$ appears as a classical control parameter $B_{\rm cl}$. However, the external field $B \to B_{\rm cl} + \delta B$ does also possess (quantum) fluctuations δB, which couple to the system of Ising spins. Therefore, we start with the following interaction Hamiltonian:

$$H_{\rm int} = \left(\sum_j \sigma_x^j\right)\otimes\delta B, \tag{36}$$

where δB denotes the bath operator. Note that this perturbation should be considered as mild, since it does not even destroy the bit-flip symmetry of the Ising model (5) and thus does not lead to leakage between the two subspaces of even and odd bit-flip symmetry (or quasiparticle number, respectively). This interaction Hamiltonian yields the same matrix elements as the nonadiabatic corrections $\langle\psi_s|\dot{H}_{\rm sys}|\psi_r\rangle$ in Eq. (10), which can therefore be calculated analogously. Insertion of $\lambda H_{\rm int}$ into Eq. (14) yields

$$\begin{aligned}\mathfrak{A}_s \approx -i\lambda\int d\omega f_s(\omega)\int_0^T dt\,\langle\psi_s(t)|\sum_j\sigma_j^x|\psi_0(t)\rangle\\ \times\exp\left\{i\left[-\omega t + \int_0^t dt'\Delta E_{s0}(t')\right]\right\}.\end{aligned} \tag{37}$$

We may also include here all relevant properties of the environment into the single-operator [compare with Eq. (19)

for the double-operator version] spectral function $f(\omega)$ of the bath

$$e^{-i\Delta\varphi_s'(t)}\,\langle\alpha_s(t)|\,\delta B(t)\,|\alpha_0(t)\rangle \equiv \int_{-\infty}^{+\infty} d\omega\, e^{-i\omega t} f_s(\omega), \quad (38)$$

where $\Delta\varphi_s'$ coincides with $\varphi_s - \varphi_0$ in Eq. (11) apart from the system's energy gap ΔE_{s0} and is typically dominated by the contribution from $H_{\rm bath}^{ss} - H_{\rm bath}^{00}$. Note that Eq. (38) is the generalization of Eq. (19) for the case that the bath state changes strongly. As a first approximation, we assume that $f(\omega)$ does not change significantly if we increase the system size N (scaling limit). After inserting the Jordan-Wigner, Fourier, and Bogoliubov transformations, the matrix element in Eq. (37) reads

$$\sum_j \langle\psi_s|\,\sigma_x^j(t)\,|\psi_0\rangle \approx \frac{2ig(t)\sin(ka)}{\mathscr{E}_k(t)}\,\langle\psi_s|\,\gamma_k^\dagger\gamma_{-k}^\dagger\,|\psi_0\rangle\,, \quad (39)$$

where the $\approx$ sign refers to the adiabatic approximation. Thus, it is only nonvanishing for excited states $|\psi_s\rangle$ containing two quasiparticles $s = (k, -k)$ with opposite momenta and, hence, we get $\Delta E_{s0} = 2\mathscr{E}_k$.

First of all, in order to have a *quantum* phase transition (or a working adiabatic quantum computer), the environment should be cold enough to permit the preparation of the system in the initial ground state such that $f(\omega)$ is only non-negligible when

$$\omega \ll 2 = \mathscr{E}_k(t=0) \quad (40)$$

holds [compare also Eq. (20)]. Therefore, we analyze the spectral excitation amplitude $\mathfrak{A}_s^\omega$ defined via

$$\mathfrak{A}_s \equiv \int d\omega\, f_s(\omega)\,\mathfrak{A}_s^\omega \quad (41)$$

in the different ω regimes in the following.

1. Intermediate positive frequencies

We may solve the time integral via the saddle-point (or stationary-phase) approximation for intermediate positive frequencies,

$$2 \gg \omega \gg \Delta E_{s0}^{\min} \approx 2|ka|. \quad (42)$$

For the exponent in Eq. (37), the saddle-point condition reads

$$\left[\frac{\partial h_k(t,\omega)}{\partial t}\right]_{t=t_*} = 0 \rightsquigarrow \omega = \Delta E_{s0}(t_*) = 2\mathscr{E}_k(t_*), \quad (43)$$

where $h_k(t,\omega) = i[-\omega t + 2\int_0^t dt'\mathscr{E}_k(t')]$ and t_* denotes the saddle points. This condition yields two saddle points shortly before and after the transition (see also Fig. 8):

$$g(t_*^\pm) = \frac{1}{2} \pm \frac{[\omega^2 - 16\sin^2(ka/2)]^{1/2}}{8\cos(ka/2)}. \quad (44)$$

The saddle-point approximation yields, for the spectral excitation amplitude defined in Eq. (41),

$$\mathfrak{A}_s^{\omega\gg 2|ka|} \approx \sqrt{\frac{\pm 32\pi i\lambda^2\sin(ka)\sin\left(\frac{ka}{2}\right)e^{2h_k(t_*,\omega)}}{\omega\dot g(t_*)g^{-2}(t_*)\sqrt{\omega^2 - 16\sin^2\left(\frac{ka}{2}\right)}}} + O\left(\frac{\lambda\dot g(t_*)}{\omega\sqrt{\omega^2-4k^2a^2}}\right), \quad (45)$$

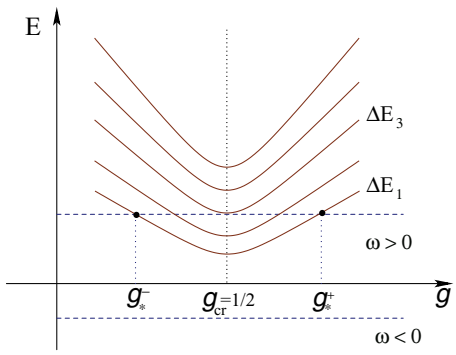

FIG. 8. (Color online) Sketch of the excitation spectrum of the Ising chain $H_{\rm sys}$ as a function of g. For a given frequency $\omega > 0$, real saddle points correspond to intersections of the (solid) energy-level curves (e.g., ΔE_1) with the (dashed) vertical ω-line, which occur shortly before (g_*^-) and after (g_*^+) the quantum phase transition at $g_{\rm cr} = 1/2$. The saddle-point approximation can only be applied if the intersection angle is large enough; that is, for the $\omega > 0$ line, it would work for ΔE_1 but not for ΔE_3, and so forth.

which depends on the interpolation dynamics $g(t)$. The minimum gap can be obtained from Eq. (34) and does indeed scale polynomially, $\Delta E_{\min} = O(1/N)$; thus,

1. For a constant-speed interpolation $g(t) = t/T$, the necessary run time for an adiabatic evolution T scales polynomially: $T = O\left(\Delta E_{\min}^{-2}\right) = O(N^2)$.
2. For adapted interpolation dynamics $\dot g(t) \propto \Delta E(t)$ or $\dot g(t) \propto \Delta E^2(t)$, however, one may achieve shorter run times of $T = O(N\ln N)$ or $T = O(N)$, respectively [10], and therefore better results for the spectral excitation amplitude (see Table I).

2. Near the minimum gap

From Eq. (45) it follows that the saddle-point approximation breaks down if ω approaches the minimum gap $w \approx \Delta E_{s0}^{\min} \approx 2|ka|$ (see Fig. 8). In this case, we may obtain an upper bound for the time integral in Eq. (37) by omitting all phases. For a constant-speed interpolation $g(t) = t/T$,

$$\mathfrak{A}_s^{\omega\approx 2|ka|} \leqslant \frac{2\lambda\sin(ka)}{T}\int_0^T dt\,\frac{t}{\mathscr{E}_k(t)} = O(\lambda N^2\omega\ln\omega). \quad (46)$$

TABLE I. Scaling of the spectral excitation amplitude $\mathfrak{A}_s^\omega$ in the saddle-point approximation ($\omega \gg 2ka$) and its upper bound ($\omega \approx 2ka$) for different interpolation dynamics $g(t)$, where $\Delta E(t) = 2\mathscr{E}_{k=\pi/(aN)}(t)$ denotes the fundamental gap. In all cases, the total excitation probability (integral over all ω and sum over all k) increases with system size N.

	$1 \gg \omega \gg 2ka$	$1 \gg \omega \approx 2ka$
$\ddot g(t) = 0$	$O(\lambda ka\omega^{-1}N)$	$O(\lambda N^2\omega\ln\omega)$
$\dot g(t) \propto \Delta E(t)$	$O(\lambda ka\omega^{-3/2}\sqrt{N})$	$O(\lambda N\ln N)$
$\dot g(t) \propto \Delta E^2(t)$	$O(\lambda ka\omega^{-2})$	$O(\lambda N)$

Similarly, one can get better results for adapted interpolation dynamics (see Table I).

3. *Positive frequencies below the minimum gap*

For positive frequencies fulfilling $0 \leqslant \omega \ll 2|ka|$, the saddle points at

$$g(t_*^{\pm}) \approx \frac{1}{2} \pm \frac{1}{8}\sqrt{\omega^2 - 4k^2a^2} \tag{47}$$

move away from the real axis and, thus, the exponent in Eq. (37) contains real terms. The constant-speed interpolation leads to

$$i\left[-\omega t_* + 2\int_0^{t_*} dt\, \mathscr{E}_k(t)\right] \approx i\eta - \left[\frac{\omega|ka|}{4} + \frac{(ka)^2}{2}\right]T, \tag{48}$$

where η is a real value. Therefore, the spectral excitation amplitude is exponentially suppressed in the adiabatic limit

$$\mathfrak{A}_s^{\omega \ll 2|ka|} = O(\exp\{-\tfrac{1}{2}T(ka)^2\}). \tag{49}$$

4. *Negative frequencies*

Finally, for negative frequencies $\omega < 0$, the saddle points collide with the branch cut generated by the square root in $\mathscr{E}_k$. In this case, we may also estimate the spectral excitation amplitude $\mathfrak{A}_s^{\omega}$ in Eq. (41) by deforming the time-integration contour into the complex plane. We assume that all involved functions can be analytically continued into the complex plane and are well behaved near the real axis. Given this assumption, we deform the integration contour into the upper complex half-plane to obtain a negative exponent, which is the usual procedure in such estimates, until reaching a saddle point, a singularity, or a branch cut (see Fig. 9). Deforming the integration contour into the lower complex half-plane would of course not change the result, but there the integrand is exponentially large and strongly oscillating such that the integral is hard to estimate. Since the integral in the complex plane is zero around path c and the integrals on paths 1 and 2 cancel each other, only paths a and b give the main contribution to the integral.

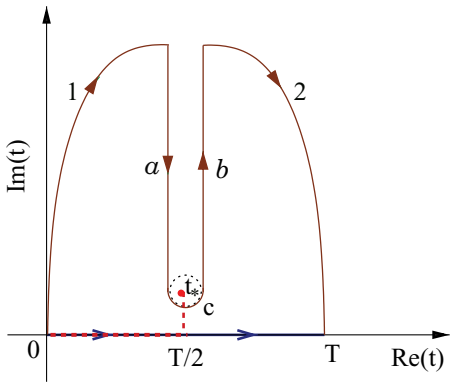

FIG. 9. (Color online) Sketch of the deformed integration contour. The original integration contour (blue bold line along the real axis) is shifted to the complex plane (curved line), where t_* indicates the singular point, $t_* = T/2 + iT/2\tan(ka/2)$. Only paths a and b contribute significantly to the integral.

Let us first consider a constant interpolation function $g(t) = t/T$ which leads to singular points

$$t_* = \frac{T}{2} \pm i\frac{T}{2}\tan\left(\frac{ka}{2}\right) \tag{50}$$

in the complex plane. Performing the time integral in the exponent of Eq. (37) acquires a large negative real term in the exponent

$$\begin{aligned}\int_0^t dt'\Delta E_{s0}(t') &= \left\{\int_0^{T/2} + \int_{T/2}^{t_*} + \int_{t_*}^{t}\right\} dt'\Delta E_{s0}(t') \\ &\approx \xi' \pm 2t^2 + \frac{i\pi T}{16}(ka)^2,\end{aligned} \tag{51}$$

where ξ' is a constant and real value. Insertion of Eq. (51) into Eq. (37) and doing some algebra yields the exponential suppression for the amplitudes in the upper complex half-plane

$$\begin{aligned}\mathfrak{A}_s^{\omega<0} &\approx \exp\left\{-\frac{\pi T}{16}(ka)^2\right\} \\ &\quad\times \int_{a,b} dt\, F(t)\exp\{i(2t^2 - \omega t + \tau)\},\end{aligned} \tag{52}$$

with $F(t) = \langle\psi_s(t)|\sum_j \sigma_j^x|\psi_0(t)\rangle$ and where τ is a real constant. Therefore, after applying the inequality

$$|\mathfrak{H}| \leqslant \int dy\, |\phi(y)| \quad \text{with} \quad \mathfrak{H} = \int dy\, \phi(y), \tag{53}$$

the amplitudes for negative frequencies are also exponentially suppressed for $g(t) = t/T$ and similarly for the other interpolations. This result can be understood in the following way. For frequencies ω below the lowest excitation energies, the energy ω of the reservoir modes is not sufficient for exciting the system via energy-conserving transitions. Hence, excitations can only occur via nonadiabatic processes for which energy conservation becomes ill defined, but these processes are suppressed if the evolution is slow enough.

An estimate of the total error probability $|\mathfrak{A}_s|^2$ introduced in Eq. (41) is obtained by performing a weighted sum of the contributions from the different ω regimes, which depends on the Fourier transform of the bath correlation function

$$\begin{aligned}|\mathfrak{A}_s^{\omega}| < &\left[\max_{\omega \gg 2|ka|}\left|\mathfrak{A}_s^{\omega \gg 2|ka|}\right|\right]\int_{2\gg\omega\gg 2|ka|} |f_s(\omega)|\, d\omega \\ &+ \left[\max_{\omega \approx 2|ka|}\left|\mathfrak{A}_s^{\omega \approx 2|ka|}\right|\right]\int_{\omega\approx|ka|} |f_s(\omega)|\, d\omega \\ &+ \left[\max_{0<\omega<2|ka|}\left|\mathfrak{A}_s^{\omega \ll 2|ka|}\right|\right]\int_0^{2|ka|} |f_s(\omega)|\, d\omega \\ &+ \left[\max_{\omega<0}\left|\mathfrak{A}_s^{\omega<0}\right|\right]\int_{-\infty}^{0} |f_s(\omega)|\, d\omega.\end{aligned} \tag{54}$$

From the results in Eqs. (45), (46), (49), and (52), it becomes obvious that, although the last two contributions in the preceding sum can be efficiently suppressed, the first two terms scale with the system size. Therefore, for the adiabatic Ising model, decoherence can only be effectively suppressed when the bath spectral function $f_s(\omega)$ only has support at frequencies below the minimum fundamental energy gap. For

a bosonic bath in thermal equilibrium, this would imply a reservoir temperature below the minimum fundamental energy gap [compare also Eq. (20)].

B. Nonuniform coupling strengths

In a realistic situation, the Ising spins are not symmetrically coupled to the environment

$$H_{\rm int} = \sum_j \sigma_x^j \otimes \delta B_j, \tag{55}$$

where δB_j now denote different operators acting on the bath Hilbert space. Insertion of Eq. (55) into Eq. (14) and evaluating the corresponding matrix element by applying the Jordan-Wigner, Fourier, and Bogoliubov transformations of Pauli matrices—given in Eqs. (26), (29), and (30)—yield

$$\begin{aligned}\mathfrak{A}_s \approx & -\frac{2i\lambda}{N}\sum_{k,k'}\int d\omega\, f^s_{k,k'}(\omega)\int_0^T dt\, u_k^*(t)v_{k'}(t)\\ & \times \langle\psi_s(t)|\,\gamma_k^\dagger\gamma_{-k'}^\dagger\,|\psi_0(t)\rangle\\ & \times \exp\left\{i\left[-\omega t+\int_0^t dt'\,\Delta E_{s0}(t')\right]\right\},\end{aligned} \tag{56}$$

where we again include all relevant properties of the environment into the spectral function $f^s_{k,k'}(\omega)$ of the bath

$$e^{-i\Delta\varphi_s'(t)}\left(\sum_j \delta B_j^{s0} e^{i(k-k')ja}\right) \equiv \int_{-\infty}^{+\infty} d\omega\, e^{-i\omega t} f^s_{k,k'}(\omega), \tag{57}$$

where $\delta B_j^{sr} = \langle\alpha_s(t)|\,\delta B_j(t)\,|\alpha_r(t)\rangle$, $\Delta\varphi_s'$ coincides with $\varphi_s - \varphi_0$ in Eq. (11) apart from the system's energy gap ΔE_{s0}, and $u_k(t)$, $v_k(t)$ are the Bogoliubov coefficients given in Eq. (33). The excitation amplitude in Eq. (56) is only nonvanishing for the excited states containing two quasiparticles $s = (k, -k')$:

$$\Delta E_{s0} = \mathscr{E}_k + \mathscr{E}_{k'}. \tag{58}$$

Insertion of u_k^*, $v_{k'}$, given by Eq. (33), into Eq. (56) yields

$$\begin{aligned}\mathfrak{A}_s \approx & \frac{i\lambda}{N}\sum_{k,k'}\int d\omega f^s_{k,k'}(\omega)\int_0^T dt\,\langle\psi_s(t)|\,\gamma_k^\dagger\gamma_{-k'}^\dagger\,|\psi_0(t)\rangle\\ & \times\frac{\mathcal{C}_{k,k'}(t)}{\mathcal{N}_{k'}}\exp\left\{i\left[-\omega t+2\int_0^t dt'\mathscr{E}_k(t')\right]\right\},\end{aligned} \tag{59}$$

where

$$\mathcal{C}_{k,k'}(t) = 4g(t)\sin(k'a)\sqrt{\frac{1}{2}+\frac{1-2g(t)\cos^2(ka/2)}{\mathscr{E}_k(t)}}. \tag{60}$$

Following the same procedure outlined earlier, we may consider different domains of ω in order to solve the time integral in Eq. (59). For the intermediate positive frequencies,

$$2 \gg \omega \gg 2|ka| \quad \text{and} \quad 2|k'a|, \tag{61}$$

the saddle-point approximation can be applied once again:

$$-\omega + 2\mathscr{E}_k(t_*) = 0, \tag{62}$$

where t_* denotes the saddle points. For the spectral excitation amplitude, the saddle-point approximation yields

$$\mathfrak{B}_s^{\omega\gg 2|ka|} = O\left(\frac{\lambda k'a}{N\sqrt{\omega\dot{g}(t_*)\sqrt{\omega^2-4k^2a^2}}}\right), \tag{63}$$

where $\mathfrak{B}_s^\omega$ is defined as following

$$\mathfrak{A}_s \approx \sum_{k,k'}\int d\omega\, f^s_{k,k'}(\omega)\mathfrak{B}_s^\omega. \tag{64}$$

The spectral excitation amplitude in Eq. (63) depends on the interpolation dynamics $g(t)$ and is very similar to Eq. (45) apart from N in the denominator. The presence of N in the denominator may cause some slowdown for the error probability (see Table I). However, the existence of many excited states—the sum over all possible k and k' in Eq. (59)—causes the growth of the error probability with the system size. If ω approaches $2|ka|$, the saddle-point approximation breaks down and we can get a similar upper bound, which is shown in Table I, by omitting all phases. With the same argument given earlier, the amplitudes are exponentially suppressed in the adiabatic limit for frequencies far below $2|ka|$. Thus, as with the discussion following Eq. (54) in the previous subsection, we may conclude, in a more general case where the coupling strength to the bath is not uniform, that the impact of decoherence for the environmental noise is very similar to the coherent reservoir and the error probability increases with the system size, unless the bath temperature lies below the minimum energy gap.

C. Perturbing the bit-flip symmetry

Unfortunately, interactions with the reservoir cannot be tailored such that one may also expect perturbations that do not reflect the bit-flip symmetry of the Ising Hamiltonian and thereby lead to leakage between the subspaces of even and odd quasiparticle numbers. Let us consider a simple case, where only one Ising spin is coupled to the environment:

$$H_{\rm int} = \sigma_z^1 \otimes \delta B. \tag{65}$$

Insertion of this interaction Hamiltonian into Eq. (14) and evaluating the corresponding matrix element yield the excitation amplitude, which is a combination of two terms

$$\mathfrak{A}_s = -\frac{i\lambda}{\sqrt{N}}\int d\omega f_s(\omega)\sum_k\left(\mathfrak{A}^\omega_{s,1}+\mathfrak{A}^\omega_{s,2}\right), \tag{66}$$

with

$$\mathfrak{A}^\omega_{s,1} \approx ie^{-ika}\int_0^T dt\frac{\beta_k}{\mathcal{N}_k}\langle\psi_s(t)|\,\gamma_{-k}^\dagger\,|\psi_0(t)\rangle\, e^{-i\omega t} \tag{67}$$

and

$$\begin{aligned}\mathfrak{A}^\omega_{s,2} \approx & e^{ika}\int_0^T dt\sqrt{\frac{1}{2}+\frac{1-2g(t)\cos^2(ka/2)}{\mathscr{E}_k(t)}}\\ & \times\langle\psi_s(t)|\,\gamma_k^\dagger\,|\psi_0(t)\rangle\exp\left\{i\left[-\omega t+2\int_0^t dt'\mathscr{E}_k(t')\right]\right\},\end{aligned} \tag{68}$$

TABLE II. Scaling of the spectral excitation amplitude $\mathfrak{A}_s^\omega$ for different interpolation dynamics $g(t)$, where $\Delta E(t) = \mathscr{E}_{k=\pi/(aN)}(t)$ denotes the fundamental gap. In all cases, the total excitation probability (integral over all ω and sum over all k) increases with system size N.

	$\mathfrak{A}_s^\omega$
$\ddot{g}(t) = 0$	$O(\lambda ka/\sqrt{N}) + O(\lambda N^{3/2})$
$\dot{g}(t) \propto \Delta E(t)$	$O(\lambda ka/\sqrt{N}) + O(\lambda\sqrt{N}\ln N)$
$\dot{g}(t) \propto \Delta E^2(t)$	$O(\lambda ka/\sqrt{N}) + O(\lambda\sqrt{N})$

where the spectral function $f_s(\omega)$ of the bath is as defined in Eq. (38). For large T, the first term $\mathfrak{A}_{s,1}^\omega$ is a Fourier transformation of some function of ω

$$\mathfrak{A}_{s,1}^\omega \approx ie^{-ika}\sin(ka)\underbrace{\left(\Sigma(\omega) - \underbrace{\int_{-T}^{0} dt\,\Xi(t)e^{-i\omega t}}_{O(1/\omega)}\right)}_{\Omega(\omega)}, \tag{69}$$

where

$$\Xi(t) = \frac{2g(t)}{\sqrt{2\mathscr{E}_k^2(t) + 4[1 - 2g(t)\cos^2(ka/2)]\mathscr{E}_k(t)}}, \tag{70}$$

$\Sigma(\omega) = \int_{-T}^{T} dt\,\Xi(t)e^{-i\omega t}$, and $\Omega(\omega)$ is some function of ω. In order to solve the time integral of $\mathfrak{A}_{s,2}^\omega$, we may employ a saddle-point approximation, which yields

$$\mathfrak{A}_{s,2}^\omega = O(T). \tag{71}$$

Thus, we can conclude that

$$\mathfrak{A}_s = \int d\omega f_s(\omega)\sum_k \underbrace{\left[O\left(\frac{\lambda ka}{\sqrt{N}}\right) + O\left(\frac{\lambda T}{\sqrt{N}}\right)\right]}_{\mathfrak{A}_s^\omega}. \tag{72}$$

The optimal run time for an adiabatic evolution T depends on the interpolation dynamics $g(t)$ (see [10]). Scaling of the spectral excitation amplitude $\mathfrak{A}_s^\omega$ for different interpolation dynamics is shown in Table II. This decoherence channel poses a significant problem to robust ground-state preparation in the Ising model: Regardless of how low the bath temperature is, the decoherent excitation probability scales with the system size. This finding is consistent with the experience that large Schrödinger cat states such as Eq. (6) are extremely sensitive to decoherence.

VI. SUMMARY

In summary, we studied the impact of decoherence due to a weak coupling to a rather general environment on first- and second-order quantum phase transitions. Since the Ising model is considered [1] a prototypical example for a second-order quantum phase transition, we expect our results to reflect general features of second-order transitions.

For the decoherence channel (36) which is always present (though possibly not the dominant channel), we already found that the total excitation probability always increases with system size N (continuum limit). Even though the probability for the *lowest* excitation $k = \pm\pi/(aN)$ can be kept under control for a bath which is well behaved in the infrared limit (see also Sec. V A4), the existence of *many* excited states $k \in \pi(1 + 2\mathbb{Z})/(aN) : |ka| < \pi$ converging near the critical point causes the growth of the error probability for large systems. This growth can be slowed down a bit via adapted interpolation schemes $g(t)$, but not stopped.

Other decoherence channels will, in the best case, display the same general behavior. For example, for $2 \gg \omega \gg |ka|$, the associated amplitudes scale as

$$\mathfrak{A}_s^\omega = O\left(\frac{\lambda\phi_s(t_*)}{\sqrt{\dot{g}(t_*)}}\right), \tag{73}$$

where ϕ_s denotes the matrix element in analogy to Eq. (39). Typically, for a homogeneous coupling to the bath, ϕ_s does not strongly depend on the system size N (for given ka and ω). Since $\dot{g}(t_*)$ decreases for $N \to \infty$ or at least remains constant, for $\dot{g}(t) \propto \Delta E^2(t)$, the total excitation probability again increases with system size N. If only a few spins are coupled via σ_j^x to the environment, the matrix element ϕ_s in Eq. (56) decreases with the system size $O(1/N)$ and then the error probability may be kept under control—for $\dot{g}(t) \propto \Delta E^2(t)$. However, ϕ_s is of order $O(1/\sqrt{N})$ for the the σ^z channel given in Eq. (66) and the Schrödinger cat states are still sensitive to decoherence.

According to the analogy between adiabatic quantum algorithms and quantum phase transitions [7,8], this result suggests scalability problems of the corresponding adiabatic quantum algorithm, unless the temperature of the bath stays below the (N-dependent) minimum gap [4] or the coupling to the bath decreases with increasing N. These problems are caused by the accumulation of many levels at the critical point $g_{\mathrm{cr}} = 1/2$, which presents the main difference to isolated avoided level-crossings (corresponding to first-order phase transitions) discussed earlier. It also causes some difficulties for the idea of thermally assisted quantum computation (see, e.g., [38]) since, in the presence of too many available levels, the probability of hitting the ground state becomes small.

Therefore, in order to construct a scalable adiabatic quantum algorithm in analogy to the Ising model, suitable error-correction methods are required. As one possibility, one may exploit the quantum Zeno effect and suppress transitions in the system by constantly measuring the energy (see, e.g., [39]). Another interesting idea involves adiabatic ground-state preparation schemes (algorithms) that provide a constant lower bound on the fundamental energy gap that does not scale with the system size. In the case of the Ising model discussed here, this is possible by increasing the complexity of the interpolation path (i.e., beyond the straight-line interpolation). Unfortunately, the simplest approach to the Ising model [40] only bounds the fundamental gap in the subspace of even bit-flip parity; that is, decoherence channels that mediate transitions between the two subspaces as, for example, in Eq. (65) will destroy the associated robustness against decoherence. Many-body interactions in the system Hamiltonian are required to resolve this problem. In this case, decoherence could be strongly suppressed for

a low-temperature bath. Of course, the generalization of all these concepts and results to more interesting cases such as the (NP-complete) two-dimensional Ising model is highly nontrivial and requires further investigations.

ACKNOWLEDGMENTS

This work was supported by the German Research Foundation (DFG) (Grant Nos. SCHU 1557/1-2,3; SCHU 1557/2-1; and SFB-TR12).

[1] S. Sachdev, *Quantum Phase Transitions* (Cambridge University, Cambridge, England, 1999).
[2] M. A. Nielsen and I. L. Chuang, *Quantum Computation and Quantum Information* (Cambridge University, Cambridge, England, 2000).
[3] E. Farhi, J. Goldstone, S. Gutmann, and M. Sipser, e-print arXiv:quant-ph/0001106 (2000).
[4] A. M. Childs, E. Farhi, and J. Preskill, Phys. Rev. A **65**, 012322 (2001).
[5] M. S. Sarandy and D. A. Lidar, Phys. Rev. Lett. **95**, 250503 (2005).
[6] A. Messiah, *Quantum Mechanics* (Wiley, New York, 1958).
[7] J. I. Latorre and R. Orús, Phys. Rev. A **69**, 062302 (2004).
[8] R. Schützhold and G. Schaller, Phys. Rev. A **74**, 060304(R) (2006).
[9] M. S. Sarandy, L. A. Wu, and D. A. Lidar, Quant. Info. Proc. **3**, 331 (2004).
[10] G. Schaller, S. Mostame, and R. Schützhold, Phys. Rev. A **73**, 062307 (2006).
[11] S. Jansen, M. B. Ruskai, and R. Seiler, J. Math. Phys. **48**, 102111 (2007).
[12] J. Roland and N. J. Cerf, Phys. Rev. A **65**, 042308 (2002).
[13] R. Schützhold, J. Low Temp. Phys. **153**, 228 (2008).
[14] J. E. Bunder and R. H. McKenzie, Phys. Rev. B **60**, 344 (1999).
[15] K. H. Fischer, and J. A. Hertz, *Spin Glasses* (Cambridge University, Cambridge, England, 1993).
[16] A. Das and B. K. Chakrabarti, Lecture Notes in Physics, Vol. 679 (Springer-Verlag, Heidelberg, 2005).
[17] G. E. Santoro, R. Martoňák, E. Tosatti, and R. Car, Science **295**, 2427 (2002).
[18] T. Kadowaki and H. Nishimori, Phys. Rev. E **58**, 5355 (1998).
[19] http://tinyurl.com/yoz77v; see also W. van Dam, Nature Physics **3**, 220 (2007).
[20] S. Mostame, G. Schaller, and R. Schützhold, Phys. Rev. A **76**, 030304(R) (2007).
[21] J. Dziarmaga, Phys. Rev. Lett. **95**, 245701 (2005).
[22] G. Schaller and R. Schützhold, Quant. Inf. Comp. **10**, 109 (2010).
[23] E. Farhi, J. Goldstone, Sam Gutmann, and Daniel Nagaj, Int. J. Quantum. Inform. **6**, 503 (2008).
[24] M. Žnidarič and M. Horvat, Phys. Rev. A **73**, 022329 (2006).
[25] R. Schützhold, M. Uhlmann, Y. Xu, and Uwe R. Fischer, Phys. Rev. Lett. **97**, 200601 (2006).
[26] R. Schützhold, Phys. Rev. Lett. **95**, 135703 (2005).
[27] G. Vidal, J. I. Latorre, E. Rico, and A. Kitaev, Phys. Rev. Lett. **90**, 227902 (2003).
[28] W. H. Zurek, U. Dorner, and P. Zoller, Phys. Rev. Lett. **95**, 105701 (2005).
[29] B. Damski, Phys. Rev. Lett. **95**, 035701 (2005).
[30] K. Sengupta, S. Powell, and S. Sachdev, Phys. Rev. A **69**, 053616 (2004).
[31] D. Patane, L. Amico, A. Silva, R. Fazio, and G. E. Santoro, Phys. Rev. B **80**, 024302 (2009).
[32] A. Fubini, G. Falci, and A. Osterloh, New J. Phys. **9**, 134 (2007).
[33] M. Tiersch and R. Schützhold, Phys. Rev. A **75**, 062313 (2007).
[34] G. Schaller and T. Brandes, Phys. Rev. A **78**, 022106 (2008).
[35] T. Brandes, Phys. Rep. **408**, 315 (2005).
[36] P. Jordan and E. Wigner, Z. Phys. **47**, 631 (1928).
[37] S. Katsura, Phys. Rev. **127**, 1508 (1962).
[38] M. H. S. Amin, Peter J. Love, and C. J. S. Truncik, Phys. Rev. Lett. **100**, 060503 (2008).
[39] A. M. Childs, E. Deotto, E. Farhi, J. Goldstone, S. Gutmann, and A. J. Landahl, Phys. Rev. A **66**, 032314 (2002).
[40] G. Schaller, Phys. Rev. A **78**, 032328 (2008).